

# **Explosive Baroclinic Instability**

**Rex J. Fleming**

**Global Aerospace, LLC**

**July 1, 2013**

## **Baroclinic instability is a fundamental mechanism for our atmosphere**

**Differential heating** between incoming solar radiation and outgoing infrared radiation causes a pole to equator temperature gradient and produces a growing supply of zonal mean available potential energy

The zonal wind, developing to geostrophically balance that temperature gradient, becomes baroclinically unstable.

The resulting baroclinic waves (eddies) transport warm air northward /cold air southward

At the same time the eddy available potential energy is converted into eddy kinetic energy by the vertical motions within the eddies -- this helps maintain the kinetic energy of the atmosphere against frictional dissipation

While the heat transported northward may balance or even temporarily exceed the radiation deficit, various processes (friction , thermal conductivity, radiation to space, etc.) damp the baroclinically unstable waves and the cycle is eventually repeated

**Phil Thompson (1987) and (1988) provided an important pedagogical approach to nonlinear baroclinic instability, crystallizing the **vacillation nature of baroclinic instability**; and whose **formula for the period of that vacillation**, as a function of differential heating and dissipation remains valid today**

In a third unpublished paper, he referred to his low-order general circulation model as the **STYX** model – he did not mention **chaos** in any of the three papers, but this model produces **chaos** (due to S.I.C.) in addition to vacillation

$$d X(1) / d \tau = -LR X(2) - LD X(1) + H \quad (1)$$

$$d X(2) / d \tau = X(1) X(3) - D X(2) - R X(4) \quad (2)$$

$$d X(3) / d \tau = X(1) X(2) - D X(3) \quad (3)$$

$$d X(4) / d \tau = R X(2) - D X(4) \quad (4)$$

**S** = X(1) = mean zonal shear (or mean horizontal temperature gradient)

**T** = X(2) = net poleward heat transport averaged over a full wavelength

**Y** = X(3) = mean meridional kinetic energy

**X** = X(4) = cross-correlation between temperature and geopotential

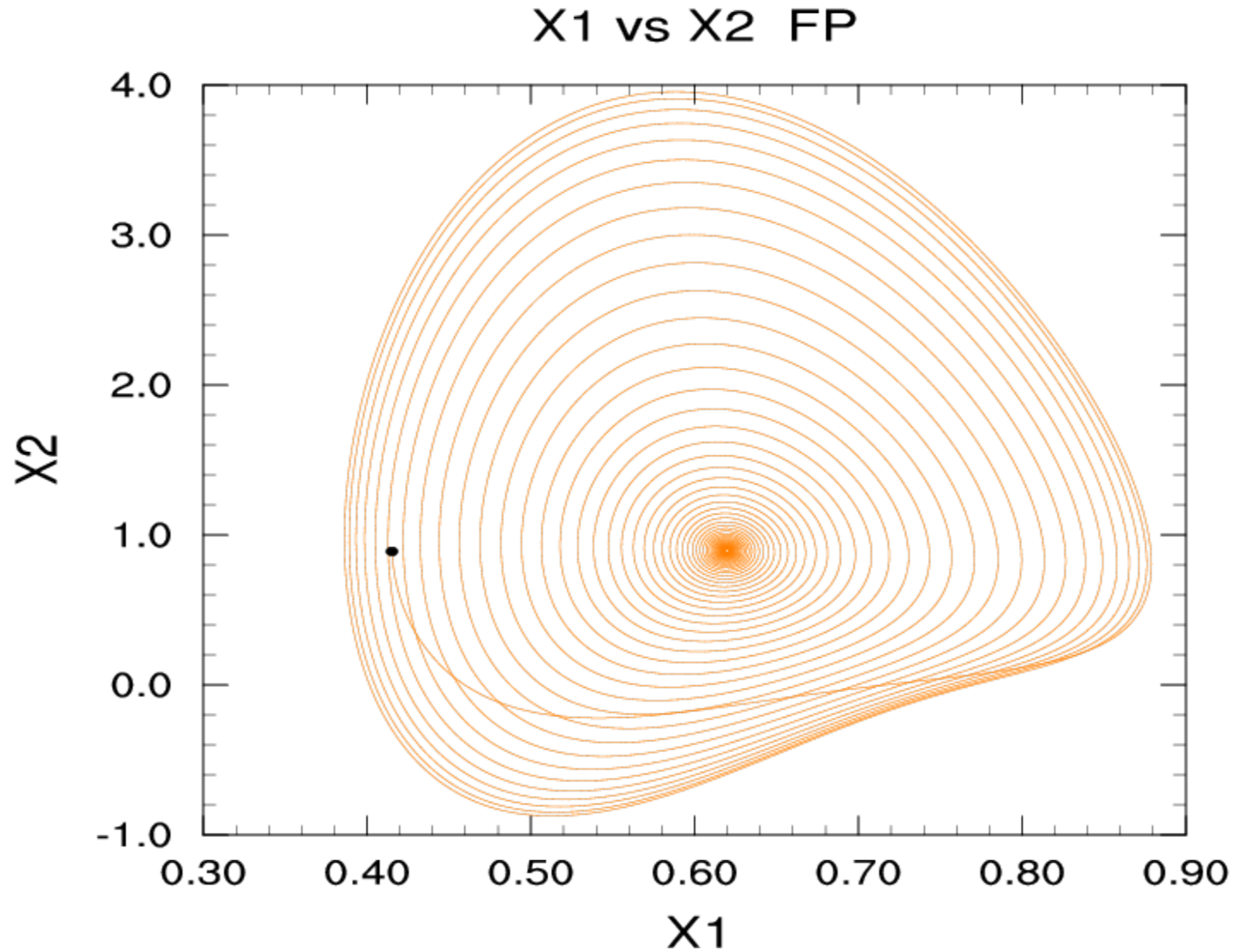


Figure 1. X1 vs X2 Vacillation / Fixed Point (FP) {run = (100, 17, 50, 50); this nomenclature explained later.} Initial X(1) = 67% of FP value

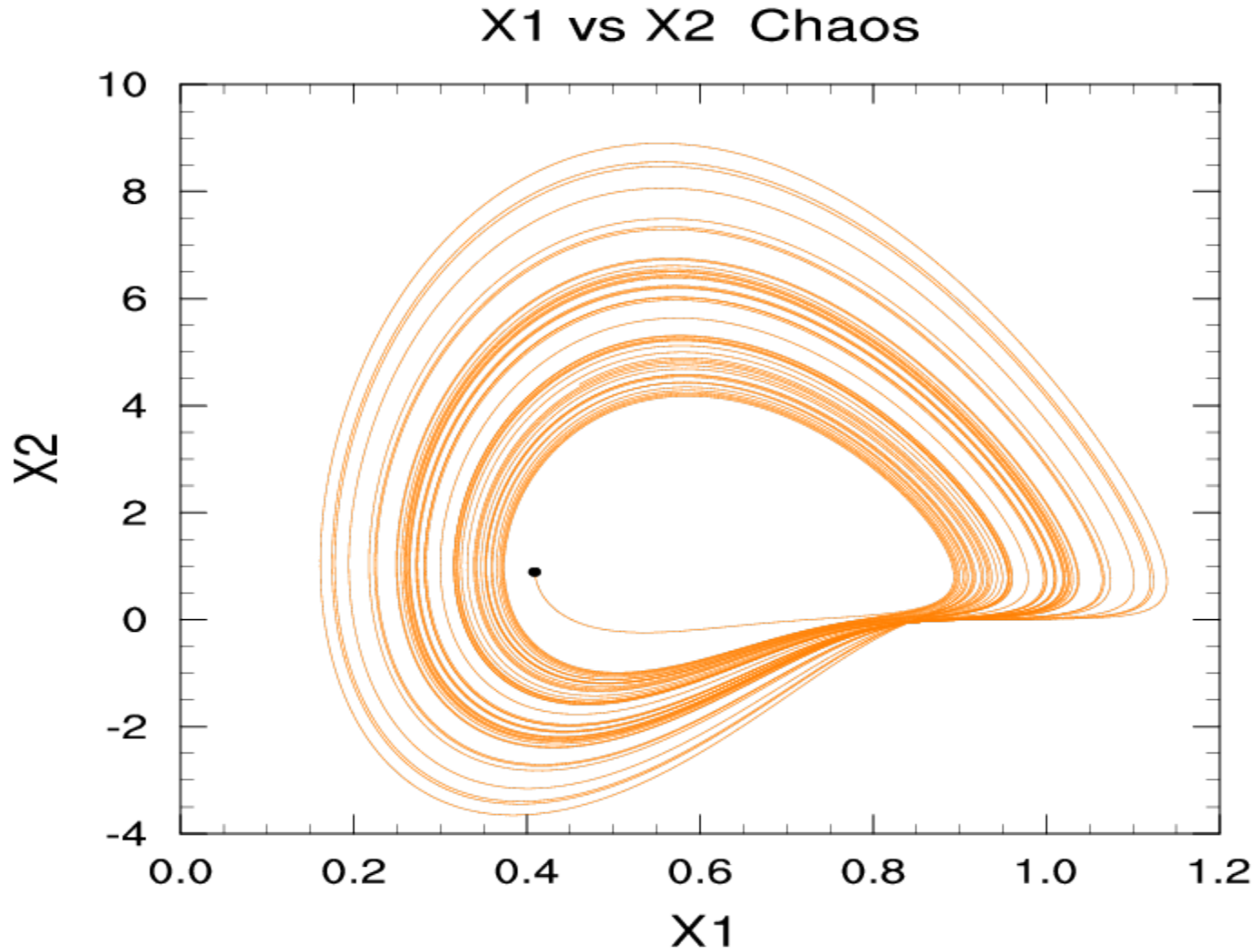


Figure 2. X1 versus X2 **Chaos run (100, 16, 50 ,50)** Initial  $X(1) = 66\%$  of its fixed point value. The Fixed Point solution started with **67%**

## Nomenclature for identifying initial conditions

The equilibrium solutions of (1) to (4), with the time tendencies set to zero, provide the fixed points:

$$X(1)_0 = (R^2 + D^2)^{1/2} = 0.61965 = X1FP$$

$$X(2)_0 = (H / L R) - (D X(1)_0 / R) = 0.89600 = X2FP$$

$$X(3)_0 = X(1)_0 X(2)_0 / D = 2.74855 = X3FP$$

$$X(4)_0 = R X(2)_0 / D = 2.59840 = X3FP$$

A caption for all runs will be of the form ( IH, ISET, JSET, KSET ) where:

$H = ( IH / 100 ) ( H_{\text{original}} )$  where  $H_{\text{original}}$  = current value of differential heating

$$X(1) = X1FP + [( ISET - 50.0 ) / 100.0 ] (X1FP)$$

$$X(2) = X2FP + [ (JSET - 50.0) / 100.0 ] (X2FP)$$

$$X(3) = X3FP + [( KSET - 50.0 ) / 100.0 ] (X3FP)$$

An initial condition of current heating and all fixed points would be ( 100, 50, 50, 50)

An initial conditional for  $X(1) = 50\%$  of its FP value would be ( 100, 0, 50, 50)

The range of  $X(1)$  from 0 to twice its FP value is given by the range ISET = - 50 to 150

# T87 model: A single unstable baroclinic wave interacting with the zonal mean shear flow, maintained against friction by differential heating

Physical basis: two-level quasi-geostrophic model in a  $\beta$ -plane channel.

The model produced quite accurate values of the mean vertical shear, the meridional velocities at the two levels, and the vacillation period of  $\sim 23$  days – close to that seen in the summer hemisphere

Symbol	Value	
$t = \text{time}$	$(k / \beta) \tau$	$k = \text{wavenumber for marginal instability} = 1.228 \times 10^{-6} \text{ m}^{-1}$ ; from $k = 2^{-1/4} k_R$ $\beta \sim 10.78 \times 10^{-12} \text{ m}^{-1} \text{ s}^{-1}$ time = [nondimensional time ( $\tau$ )] x [ $\sim 1.3$ days ]
$U$ or $v$ = velocity	$(\beta / k^2)$ $U$ or $v$	Velocity = [ $U$ or $v$ nondimensional ] x [ $7.15 \text{ m s}^{-1}$ ]
$R$	<b>0.5858</b>	$R = (k_R)^2 / [ (k_R)^2 + k^2 ]$ $k_R = \text{inverse square of Rossby radius of deformation}$
$L$	<b>0.065</b>	$L = \Pi^2 / k^2 W^2$ ; $W = \text{channel width} = 1 \times 10^7 \text{ m}$
$D$	<b>0.202</b>	$D = 2 C k^3 / \beta$ ; $C = \text{coefficient of eddy viscosity and eddy conductivity}$
$H^*$	<b>0.042253</b>	$H^* = 2 N^{1/2} H$ ; $H = 0.051$ $N = [ (k_R)^2 - k^2 ] / [ (k_R)^2 + k^2 ] = 0.1716$

Table 1. Scaling parameters and constants used in T87, T88, and this study

Thompson's formula for the frequency of vacillation (T88), rescaled and put in terms of just H/D, can be expressed as:

$$\sigma = [ LR X3FP ]^{1/2} = [ LR (X1FP) (X2FP / D) ]^{1/2} = [ 0.61965 (H/D) - 0.02496 ]^{1/2}$$

With the time step = 0.01, the nondimensional period was between 19.42 and 19.43 for H = 100. The period  $T = 2\pi / \sigma$ , and from the equation above  $\sigma = 0.32350$ , making the period from the formula  $T = 19.422$  – very accurate compared to the nonlinear calculation

Holding D fixed and increasing H shows that the formula is accurate for all H/D

IH	Iteration Period of Max X(2)	Period Calculated by T88, his Eq (25)	Period in days	Initial Max of X(2)	Final Fixed Point Value of X(2)
100	1942 19.42	19.422	25.25	3.8080	0.8960
120	1739 17.39	17.388	22.60	3.9613	1.1179
140	1589 15.89	15.883	20.65	4.2016	1.3399
160	1471 14.71	14.711	19.12	4.4758	1.5618
180	1377 13.77	13.765	17.89	4.7663	1.7837
200	1298 12.98	12.981	16.88	5.0651	2.0057

Table 2. Vacillation / fixed point (FP) solutions, as function of H. Runs = (IH, ISET, 50, 50)

**But why the chaos– first we have to find the attractors in this model!**

**The equilibrium solutions of (1) – (4), with the time tendencies set to zero give:**

$$L R X(2)_0 + L D X(1)_0 = H \quad (5)$$

$$X(1)_0 X(3)_0 - D X(2)_0 - R X(4)_0 = 0 \quad (6)$$

$$X(1)_0 X(2)_0 - D X(3)_0 = 0 \quad (7)$$

$$R X(2)_0 - D X(4)_0 = 0 \quad (8)$$

Re-arranging these yields the equation:  $X(2)_0 [ X(1)_0^2 - ( R^2 + D^2 ) ] = 0 \quad (9)$

**There are three possible solutions to (9)**

**The 1st is the stable FP solution  $X(1)_0 = ( R^2 + D^2 )^{1/2}$  when  $H > H_{\text{Critical}}$  (more later)**

**The 2<sup>nd</sup> is the unstable solution  $X(1)_0 = - ( R^2 + D^2 )^{1/2}$  and unphysical (if X(1) large “~~≠~~” then (from above) X(2) is positive and X(3) is negative, but “~~≠~~” kinetic energy not real**

**The 3<sup>rd</sup> possible solution to (9) is  $X(2)_0 = 0$ ; from above, this implies  $X(3)_0$  and  $X(4)_0 = 0$**

**This is zonal motion where the north-south temperature gradient by differential heating is exactly balanced by eddy conduction of heat by motions of subsynoptic scale – no baroclinic instability is involved. The stability of this solution is examined next**

The equations below are perturbation equations for (1) – (4) with  $X(2)_0 = X(3)_0 = X(4)_0 = 0$

$$\begin{array}{rcl}
 (\sigma + LD) X(1)' + LR X(2)' & & = 0 \\
 (\sigma + D) X(2)' - X(1)_0 X(3)' + R X(4)' & & = 0 \\
 - X(1)_0 X(2)' + (\sigma + D) X(3)' & & = 0 \\
 - R X(2)' + (\sigma + D) X(4)' & & = 0
 \end{array}$$

where the primes denote infinitesimal departures from equilibrium values

The linear homo. Eqs. have nonzero solutions only if determinant of coefficients = 0

$$\Delta = \begin{vmatrix}
 (\sigma + LD) & LR & 0 & 0 \\
 0 & (\sigma + D) & -X(1)_0 & R \\
 0 & -X(1)_0 & (\sigma + D) & 0 \\
 0 & -R & 0 & (\sigma + D)
 \end{vmatrix}$$

Expanding, factoring out the two roots  $\sigma = -LD$  and  $\sigma = -D$  gives: { note:  $X(1)_0 = H/LD$  }  
 $\sigma = -D \pm [H^2 / L^2 D^2 - R^2]^{1/2}$  Thus, if  $\sigma$  is positive, amplification, and zonal solution is unstable

$$H_{\text{Critical}} = L D (R^2 + D^2)^{1/2} = (0.065) (0.202) (0.61965) = 0.00814$$

But today's H is > 5 times  $H_{\text{Critical}}$  Thus, the zonal solution is always unstable

There is battle between these two attractors: (the stable FP solution) and the (unstable zonal solution) that will lead to chaos

**There is a broad landscape of possible initial conditions leading to chaos -- but lets first look at just the role of the mean zonal shear  $X(1)$  in forming chaos**

One might guess that initial states **near** the (the FP attractor) would produce FP solutions, and those near zonal flow conditions (the unstable zonal attractor) might produce chaos. **But the appearance of chaos is more complicated than that; Below Runs = (IH, ISET, 50, 50)**

IH	Lower FP ISET Range	Lower Chaos ISET Range	Upper FP Range about ISET = 50	Upper Chaos ISET Range
100	- 50 to - 1	0 to 16	17 to 96	97 to 150
120	- 50 to - 7	- 6 to 11	12 to 104	105 to 150
140	- 50 to - 13	- 12 to 6	7 to 113	114 to 150
160	- 50 to - 19	- 18 to 1	2 to 121	122 to 150
180	- 50 to - 25	- 24 to - 4	- 3 to 129	130 to 150
200	- 50 to - 31	- 30 to - 9	- 8 to 138	139 to 150

**For IH = 100, the FP range is broad about ISET = 50, ranging from ISET = 17 to 96, or from 67% of the FP to 146% of the FP value of  $X(1)$  – somewhat consistent with our guess; and there is a lower chaos range and an upper chaos range on both sides of the  $X(1)$  FP range.**

**However, there is another FP range on the far left of Table 4 – not consistent with our guess. The increased IH is making the dynamic system more stable: (1) squeezing out the chaos (broadening FP range about ISET = 50); (2) lowering the range of chaos in the Lower Chaos Range; and (3) eliminating chaos at the Upper Chaos Range**

From the previous Table for ( $IH = 100$ ) we have conditions at the boundary points  $ISET = -1$  (FP) and  $ISET = 0$  (Chaos) at the **left side** of the chaos range, and the points  $ISET = 16$  (Chaos) and  $ISET = 17$  (FP) at the **right side** of the chaos range

There is **no symmetry** at the chaos boundary:  $ISET = 0$  and  $JSET = 0$  to  $45$  gives FP solutions, but  $ISET = 16$  and  $JSET = 0$  to  $150$  gives chaos

ISET X(1)	JSET Range X(2)	KSET Range X(3)	Solution Type
- 1	0 to 150	50	Fixed Point
0	0 to 45	50	Fixed Point
0	46 - 81	50	Chaos
0	46	0 to 50	Chaos
0	46	51 to 60	Fixed Point
0	46	61 to 150	Chaos
0	81	0 to 50	Chaos
0	81	51 to 67	Fixed Point
0	81	68 to 150	Chaos
16	0 to 150	50	Chaos
17	14 to 99	50	Fixed Point

There is **no symmetry** at the boundary of JSET ( $46 \neq 81$ ) as KSET is erratic on the results

We will not explore this broad landscape in detail, rather we will show exactly why and where the chaos forms from first principles of stability analysis; ---- but first ----- >>

**It is important to emphasize the following facts:**

**This simple model contains all the elements of baroclinic instability; it will be further shown that it contains FP solutions, vacillation, limit cycles, and chaos.**

**All of these features occur in our real atmosphere, but are constantly changing due to a variety of nonlinear processes (changing dynamics and changing differential heating) which include wave-wave interaction, coastal air sea interaction, changing seasons, etc.**

**This variability assures us that the range of initial conditions for the atmosphere is vast, perhaps exceeding the range of initial conditions explored in this study**

**On the other hand, that same variability implies that none of these features or essential elements remain stationary in nature – though they persist in this simple model once they form**

**Despite the model's shortcomings, it is capable of explaining these features and exactly why they form**

**We want to examine the stability of the system of equ. (1) - (4) at every time step**

**Consider an infinitesimal departure for each variable as a primed quantity**

**The variables themselves are considered constant at that instant.**

**We seek solutions of the form:**

$$[ X(1)' , X(2)' , X(3)' , X(4)' ] = [X(1) , X(2) , X(3) , X(4) ] e^{\sigma T}$$

The linear equations become:

$$(\sigma + LD) X(1)' + LR X(2)' = 0$$

$$-X(3) X(1)' + (\sigma + D) X(2)' - X(1) X(3)' + R X(4)' = 0$$

$$-X(2) X(1)' - X(1) X(2)' + (\sigma + D) X(3)' = 0$$

$$-R X(2)' + (\sigma + D) X(4)' = 0$$

**These equations are linear and homogeneous; they have nonzero solutions only if the determinant  $\Delta$  of their coefficients is equal to zero**

Dividing out the common factor (  $\sigma + D$  ), which implies  $\sigma = -D$  is one solution to the equation and rearranging terms gives:

$$\sigma^3 + [2D + LD] \sigma^2 + \{ [L(2D^2 + RX(3))] + [R^2 + D^2 - X(1)^2] \} \sigma + L [RX(1)X(2) + RD X(3) + R^2 D + D^3 - D X(1)^2] = 0$$

**This is a cubic equation in  $\sigma$** ; our equation is in the classic form of

$$X^3 + A_1 X^2 + A_2 X + A_3 = 0;$$

where the **A terms** are:

$$A_1 = 2D + LD \quad (\text{which is composed only of constants})$$

$$A_2 = L [(2D^2 + RX(3))] + [R^2 + D^2 - X(1)^2]$$

$$A_3 = L [RX(1)X(2) + RD X(3) + R^2 D + D^3 - D X(1)^2]$$

## We need to examine the roots of the cubic equation

$$Q = [ A_1^2 - 3 A_2 ] / 9$$

$$R = [ 2 A_1^3 - 9 A_1 A_2 + 27 A_3 ] / 54$$

The value of  $[ Q^3 - R^2 ] = \text{Test}$  determines if there are **three real roots** or **one real root** and **two complex conjugate roots**

---

If  $[ Q^3 - R^2 ] < 0$  then **one real** and **two complex**

$$R1 = A + B - A_1/3$$

$$R2 = 0 = R3 = 0.0$$

Two roots:  $(R_{PART} + i C_{PART})$  and  $(R_{PART} - i C_{PART})$

If  $[ Q^3 - R^2 ] \geq 0$  then **three real roots**

$$\Phi = \text{Arc cos} [ R / (Q^3)^{1/2} ]$$

$$\text{Temp} = -2 Q^{1/2}$$

$$Q1 = \cos (\Phi / 3) \quad Q2 = \cos (\Phi + 2 \Pi / 3) \quad Q3 = \cos (\Phi + 4 \Pi / 3)$$

$$R1 = \text{Temp} * Q1 - A_1/3$$

$$R2 = \text{Temp} * Q2 - A_1/3$$

$$R3 = \text{Temp} * Q3 - A_3$$

**Usually large Negative**

**Always Positive**

**Small pos. or neg.**

The real parts of the roots (the TRACE) is always **constant**– and in this case, always **negative** – so the system is a restricted or a **bounded dissipative dynamic system** – there can never be runaway baroclinic instability

$$\text{If Test} < 0: R1 + 2 RPART = (A + B - A_1/3) + 2 [ - 0.5(A + B) - A_1/3 ] = - A_1$$

$$\text{If Test} \geq 0: R1 + R2 + R3 = \text{Temp}^* (Q1 + Q2 + Q3) + (3)( - A_1/3)$$

if  $(Q1 + Q2 + Q3) = 0.0$ , and they always do, then  $R1 + R2 + R3 = - A_1$

For our cubic equation , the TRACE =  $- A_1 = - (2D + LD) = - 0.417130$

---

This occurs at every iteration; even though the system is bounded, there remains the **stable attractor of the fixed points**, and the **unstable attractor of zonal flow**.

We will show the **sequence of events** of the root changes through a complete chaos cycle – though the values may change in subsequent cycles, the **sequence of events** will remain the same for all the chaos cycles.

First we look at some actual chaos details in diagram form

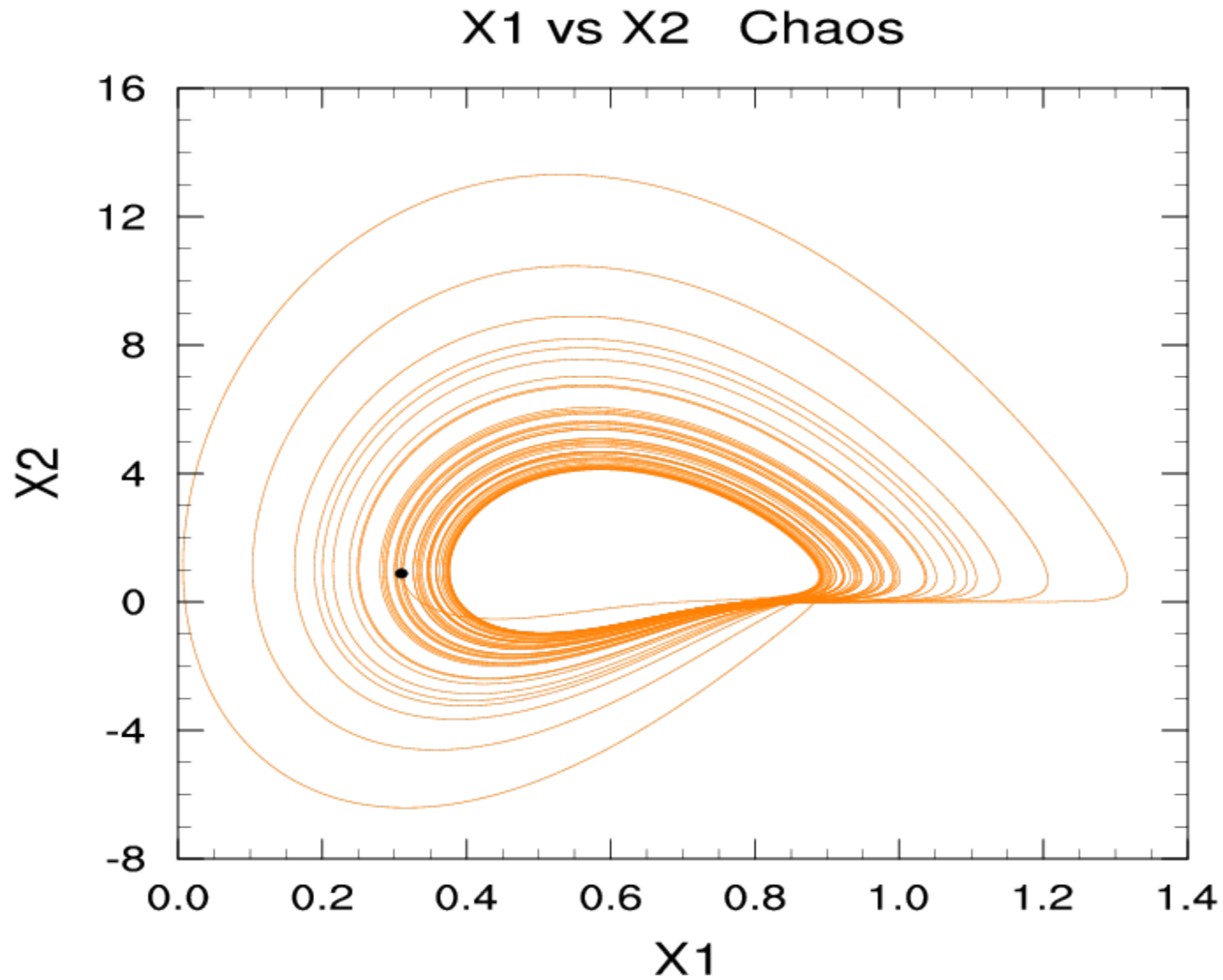


**Figure 3. X1 versus X2 Chaos run (100,0,50,50) Iterations = 100,000**

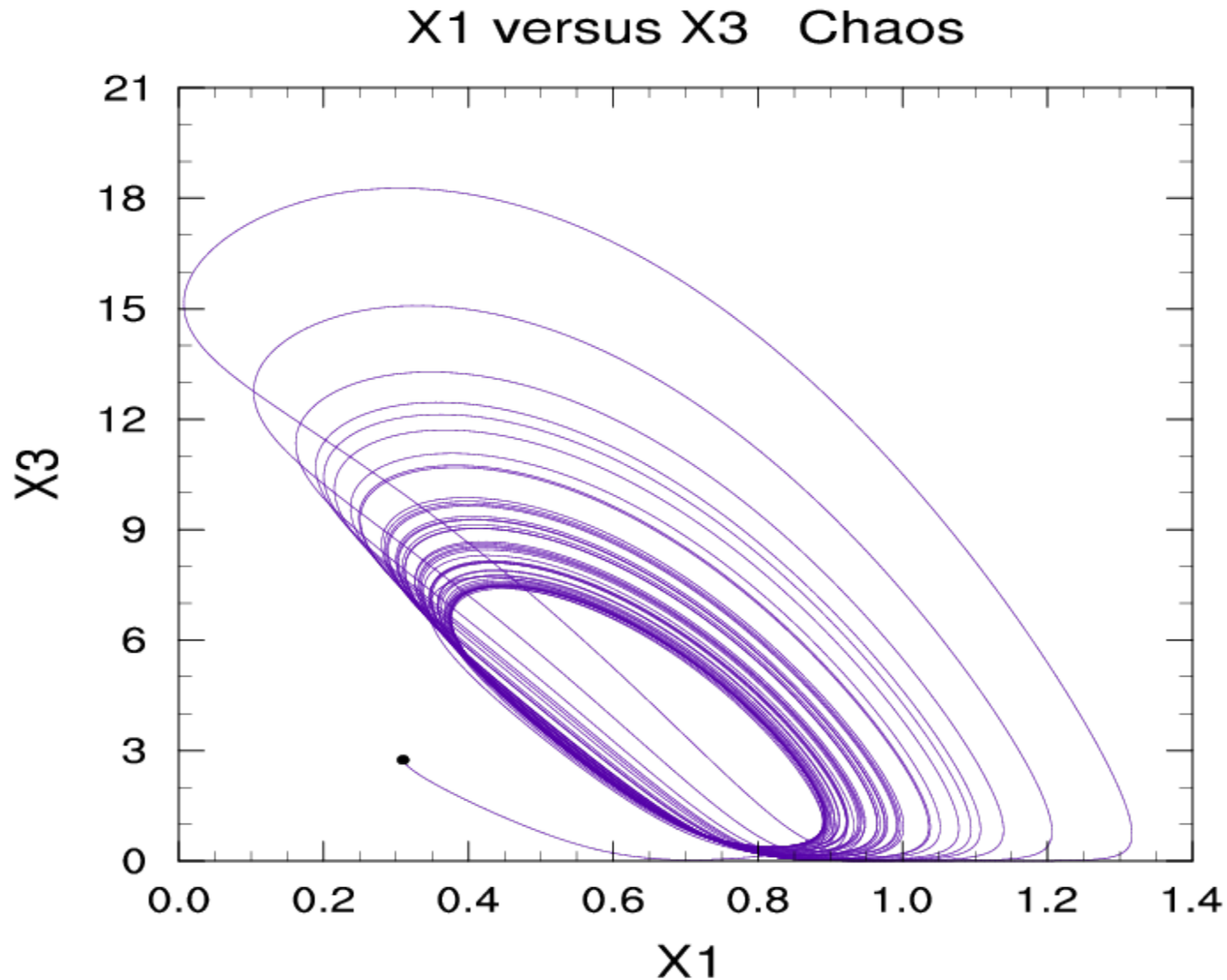
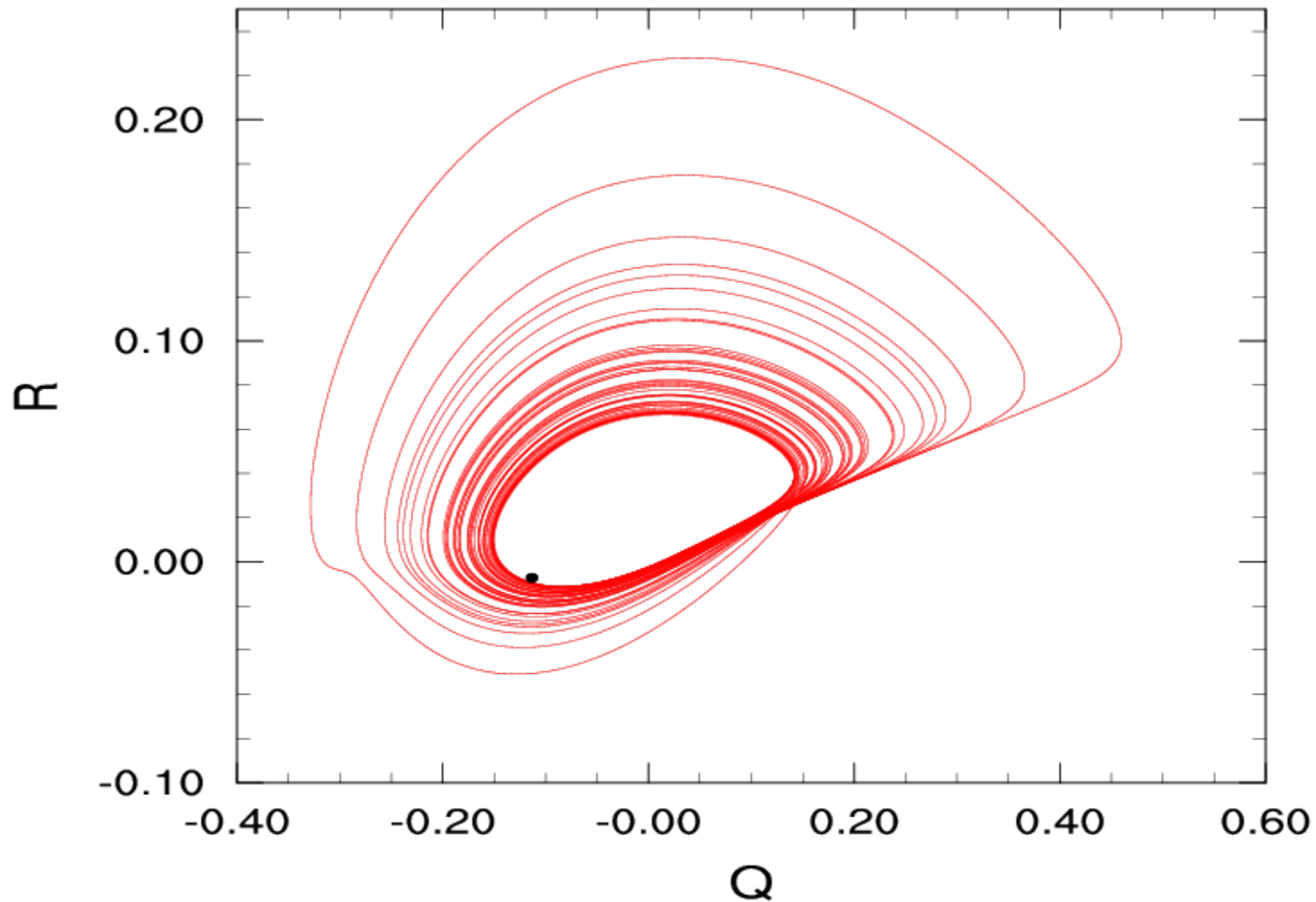


Figure 4. X1 versus X3 Chaos run (100, 0, 50, 50) Iterations = 100,000  
Note that  $X(3)$  is always positive as kinetic energy should be

## Q versus R Chaos



**Figure 5. Q versus R Chaos run (100, 0, 50, 50) Iterations = 100,000**  
**There is much wider range of Q compared to R**

## X1 vs R1 Chaos

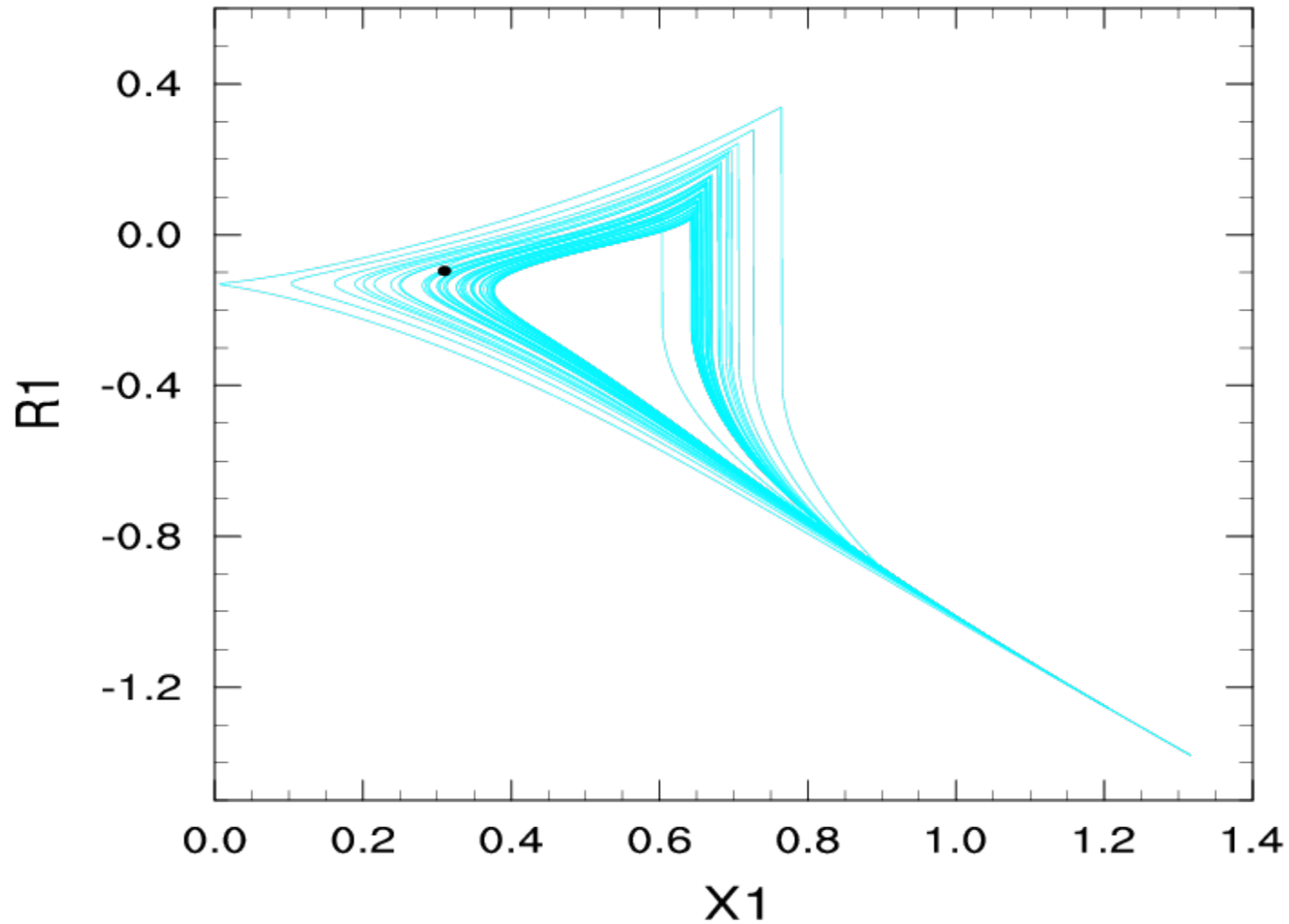


Figure 6. X1 versus R1 Chaos run (100, 0, 50, 50) Iterations = 100,000  
R1 has a strong negative correlation with X1 – controlling its magnitude

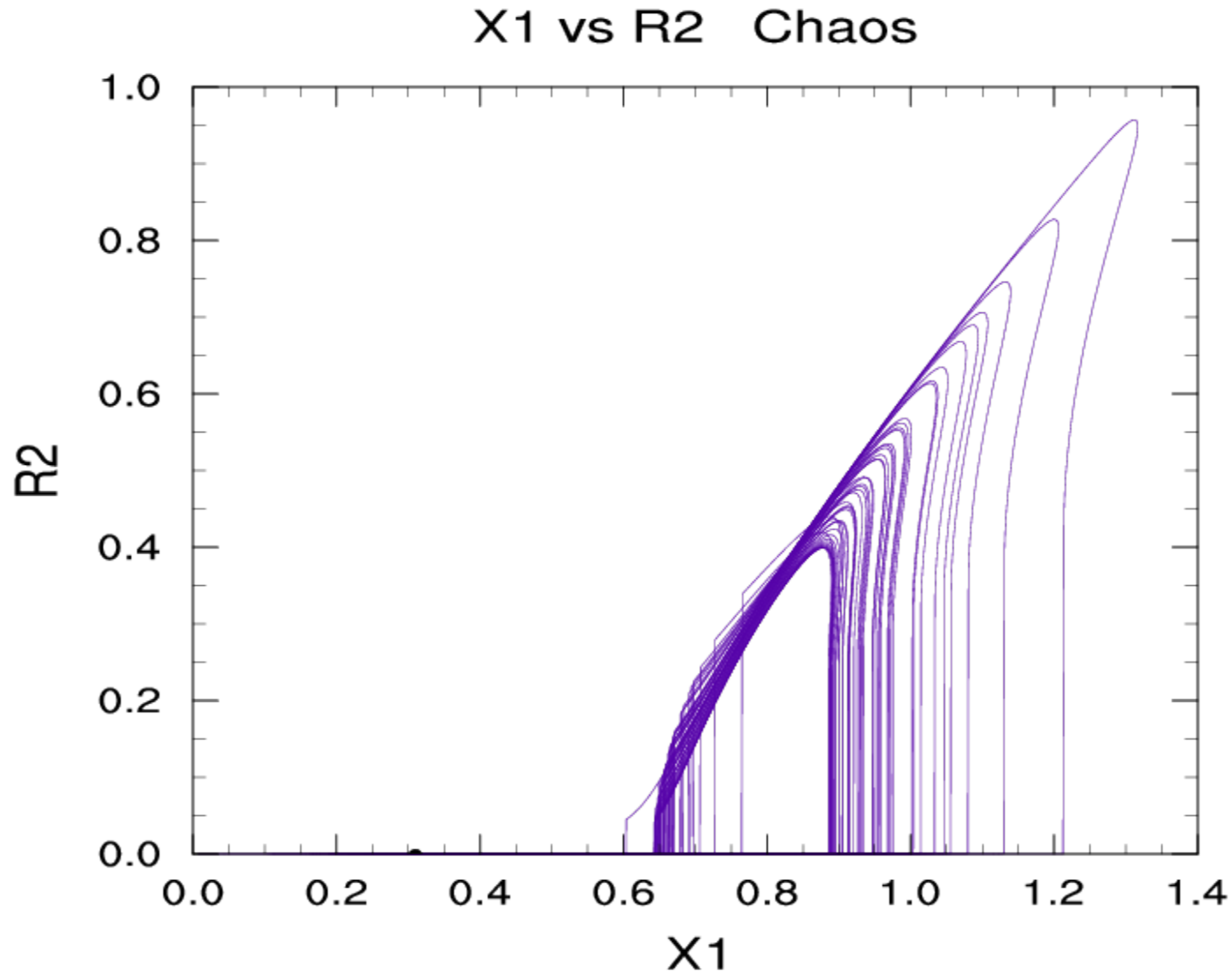


Figure 7.  $X1$  versus  $R2$  Chaos run (100, 0, 50, 50) Iterations = 100,000  
 $R2$  emerges from and goes back to zero in a baroclinic chaos cycle, as  $Q^3 - R^2$  changes from negative to positive and back to negative again

## The first cycle of a chaos run (100, 0, 50, 50)

Iteration	X(1)	R1	R2	R3	RPART	X(2)
0	.3196	-.09924	0	0	-.15895	.8960
1	.3197	-.09892	0	0	-.159104	.8878
643	.6045	<b>.04552</b>	0	0	-.23133	-.1954
		<b>Q<sup>3</sup> - R<sup>2</sup></b>	goes from	(-) to (+)	<b>three real</b>	<b>roots</b>
644	.6049	-.24436	.04584	-.21861	0	-.1944
1639	.9029	-.88903	<b>.44226</b>	.02964	0	.3888
1783	<b>.9029</b>	<b>-.90536</b>	.40773	.08050	0	.7940
1878	.9075	-.89511	.24578	<b>.23220</b>	0	1.2745
		<b>Q<sup>3</sup> - R<sup>2</sup></b>	goes from	(+) to (-)	<b>1 real root</b>	<b>2 complex</b>
1979	.9073	-.89488	0	0	.23887	1.2808
2269	.5829	-.45709	0	0	.01998	<b>4.5417</b>

After **R2** becomes a maximum, X(1) and X(2) have a max 144 and 630 iterations later

In most FP runs, there are **never** three real roots

It is clear that **R2** plays the major role in producing chaos and it will be investigated

## Find the critical value of R2 that produces chaos

For three real roots  $[Q^3 - R^2] \geq 0$  and Q must be positive since raised to the 3<sup>rd</sup> power

$$Q = 0.1456 - 0.0127 X(3) + X(1)^2$$

X(1) dominates Q and the always positive X(3) has a small role in lowering Q

$$R = -0.02185 + 0.0012 X(3) + 0.01904 X(1) X(2) + 0.06295 X(1)^2$$

Larger X(2) (it is increased by increasing H) makes the system more stable

Larger X(3) increase R, making system more stable with higher R and lower Q

---

From the previous Table for IH = 100, one sees that (100, 0, 45, 50) produces a fixed point solution and (100, 0, 46, 50) produces chaos.

This is one such boundary to try to achieve a balance between a chaos solution and a FP solution – trying to create an “apparent” or “balanced” limit cycle

Since lowering X(3) or KSET produces a slightly less stable condition, we use (100, 0, 45, ~50) but incrementally lower X(3) from KSET = 50, until we achieve a balance between a FP and chaotic solution.

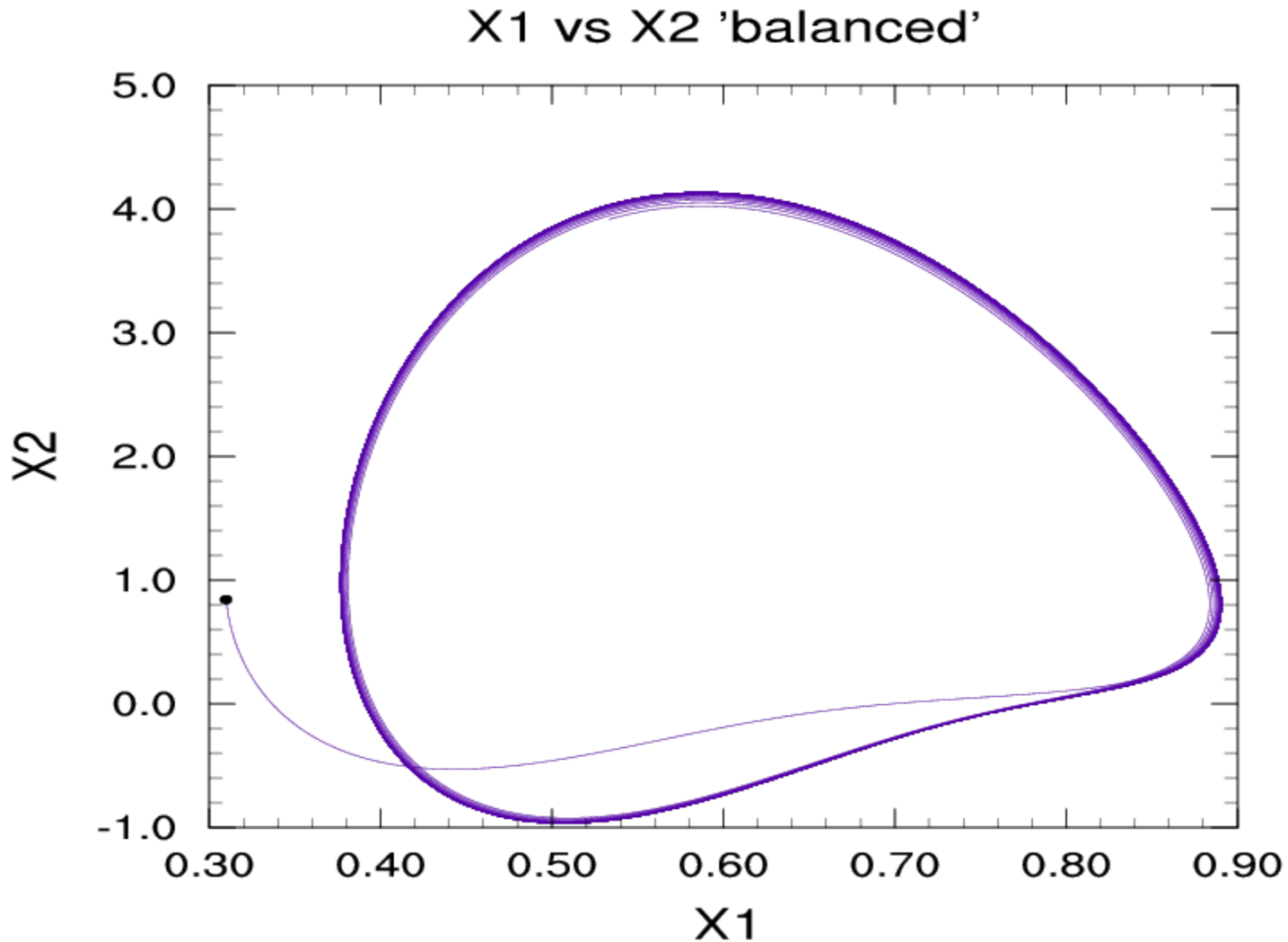


Figure 9. X1 versus X2 'balanced' run (100, 0, 45, ~ 50) Iterations = 76,000  
Here the initial maximum R2 root  $\approx 0.399\ 089$  both solutions look the same to  
76,000 iterations

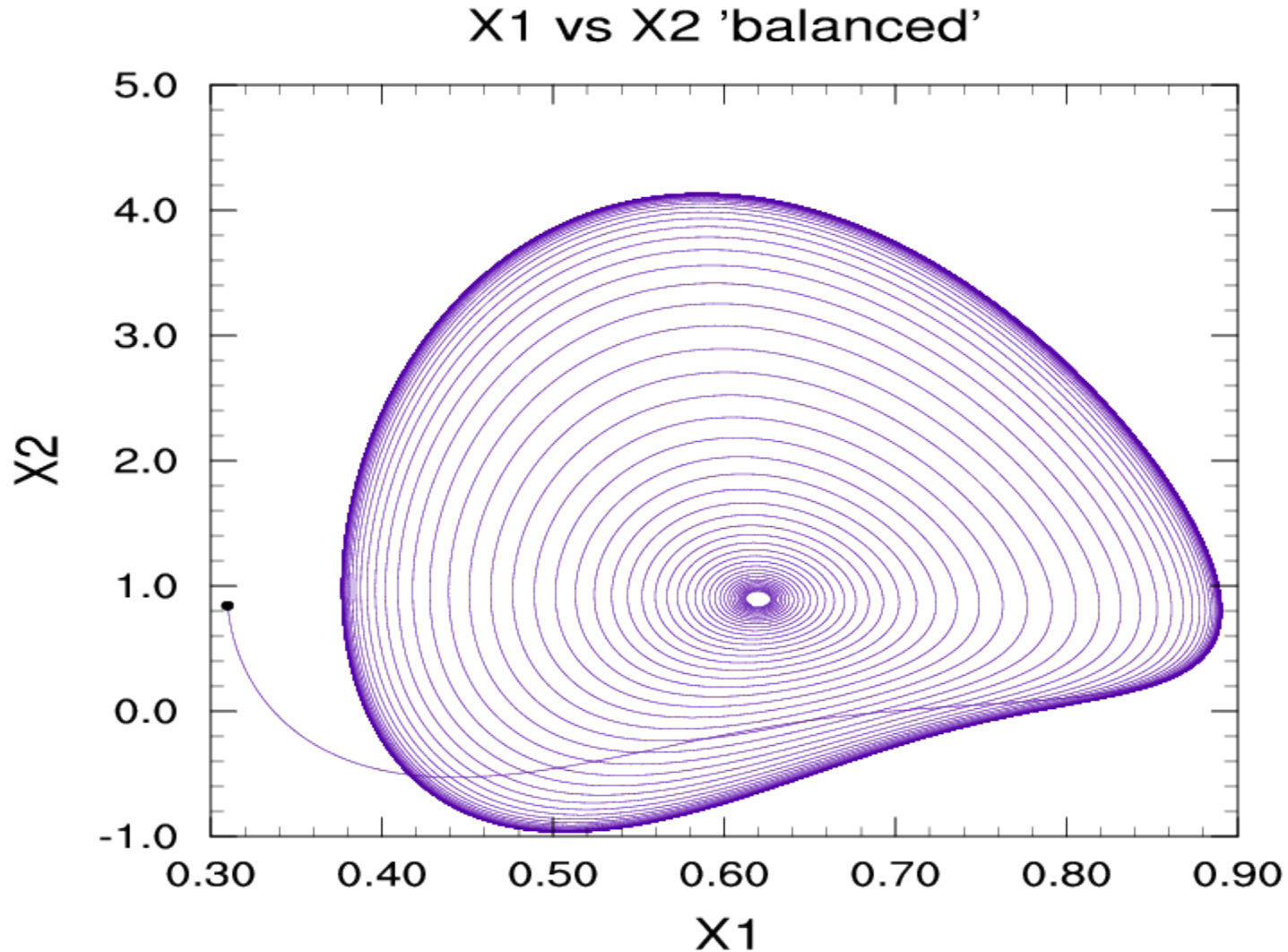


Figure 10. X1 versus X2 in “balanced/FP’ run (100, 0, 45, ~50) Iterations = 150,000  
Here the initial **maximum R2 root = 0.399 0897** and the solution vacillated to the FP

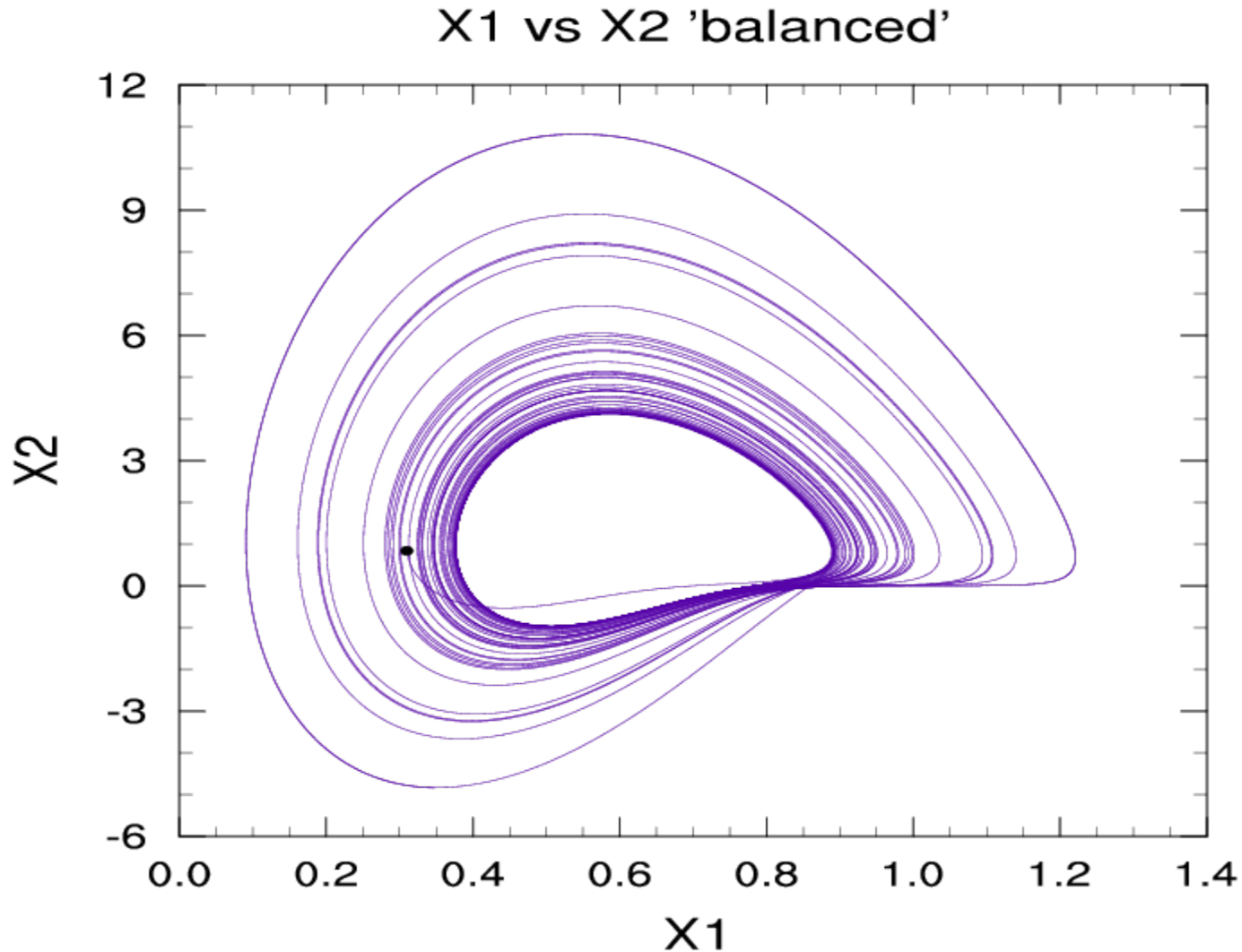


Figure 11. X1 versus X2 “balanced/Chaos run” (100, 0, 45, 49) Iterations = 150,000. Here the initial **maximum R2 root = 0.399 0899** or  $2 \times 10^{-7}$  larger than before and the solution left the “balanced” limit cycle after 76,000 iter. and proceeded to chaos.

Since increased differential heating (IH) makes the system more stable, it was expected that the critical value of R2 would go up with the more stable heating – making it harder for chaos to occur.

This is indeed the case – using a similar method to find the R2 critical values, the procedure produces the following results for higher IH

IH	Critical R2
100	0.3991
120	0.4475
140	0.4966
160	0.5452
180	0.5927
200	0.6400

For all vacillation / FP runs, the critical value of R2 is never exceeded for a given IH

For chaos, the first maximum R2 usually exceeds the critical value, but in balanced cases, it may take a few more maximum R2 values before it is exceeded, but it is always exceeded

There has been no mention of the role of X(4); it does not appear in the determination of the roots; it is part of another innocuous attractor

If one multiplies equation (2) by X(2), equation (3) by X(3), and equation (4) by X(4), and then adds these together one obtains:

$$\frac{1}{2} \frac{d}{dT} [ X(2)^2 - X(3)^2 + X(4)^2 ] + D [ X(2)^2 - X(3)^2 + X(4)^2 ] = 0$$

The solution to the above equation is:

$$[ X(2)^2 - X(3)^2 + X(4)^2 ] = [ X(2)_{(0)}^2 - X(3)_{(0)}^2 + X(4)_{(0)}^2 ] e^{-2DT}$$

For any initial state of the system, the trajectory of the phase point [X(1),X(2),X(3),X(4)] will asymptotically approach the hypersurface:

$$X(3)^2 = X(2)^2 + X(4)^2 .$$

If originally on the surface, it will stay on the surface. We chose X(2) and X(3), then make X(4) satisfy the equation  $X(3)^2 = X(2)^2 + X(4)^2$  to keep it on the surface for all runs

This is an equation for a cone; it is another attractor of the system, **but exists whether there is vacillation or chaos**

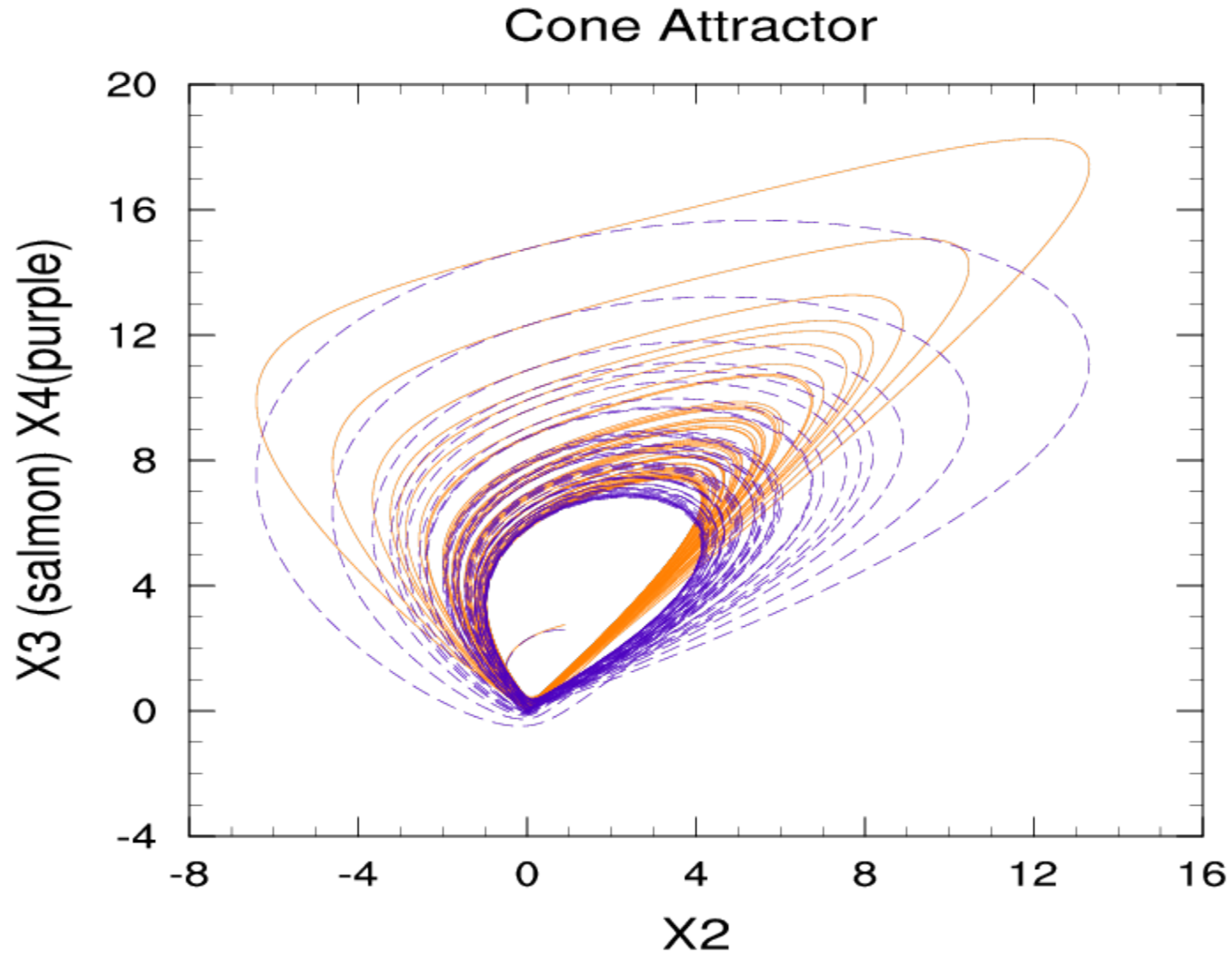


**Figure 8. The Cone Attractor in chaos run (100, 0, 50, 50)**

# Impact of increased IH on chaos and vacillation

The system is more stable with increased IH. The **R2 critical value is passed in** would-be chaos fashion and it looks like chaos for the first 10 cycles, but then the system bifurcates to **two locked-in limit cycles**.

With increased IH the **periods and amplitudes merge (at IH = 250) to a single limit cycle**. At **IH  $\geq$  356** there is no chaos. We use **IH = 300** to explain – same for all

IH	Chaos Range ( Initial ISET)	Bifurcation Point (iteration)	Frequency Range (iterations) ( + / 𐄂)	Long Cycle iterations	Short Cycle iterations	Max X(1) Long Short
200	-30 to -9	1439.5	294.5	1734	1145	1.529 1.302
205	-31 to -10	1415	263	1678	1152	1.530 1.323
210	-33 to -12	1391	230	1621	1161	1.530 1.344
220	-35 to -14	1347	156	1503	1191	1.526 1.392
230	-38 to -16	1307	51	1358	1256	1.504 1.458
240	-41 to -19	1271	3	1274	1268	1.514 1.513
<b>250</b>	<b>-43 to -21</b>	1238	<b>0</b>	<b>1238</b>	<b>1238</b>	<b>1.5479</b> <b>1.5479</b>

## X1 versus R Chaos/Limit Cycle

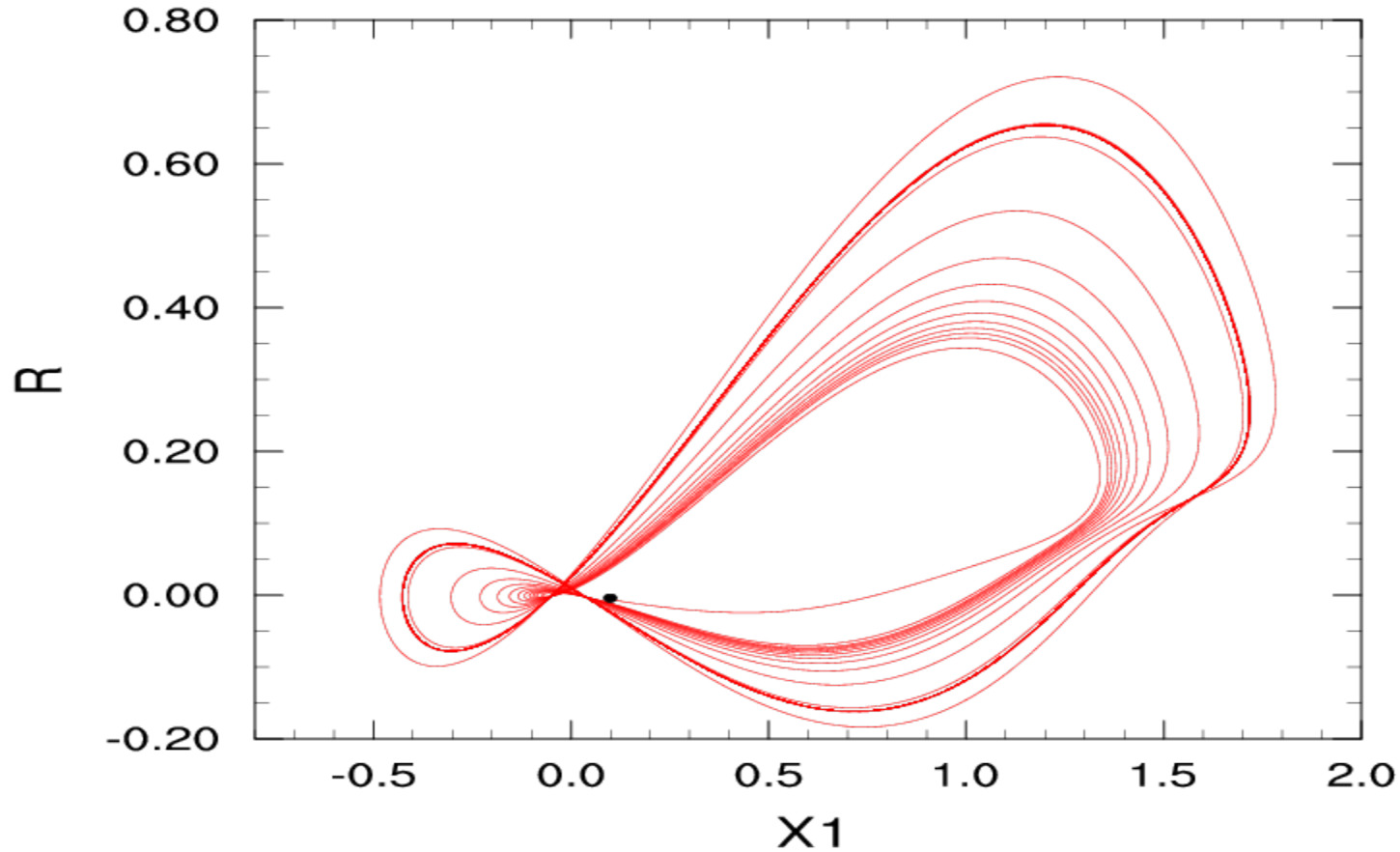
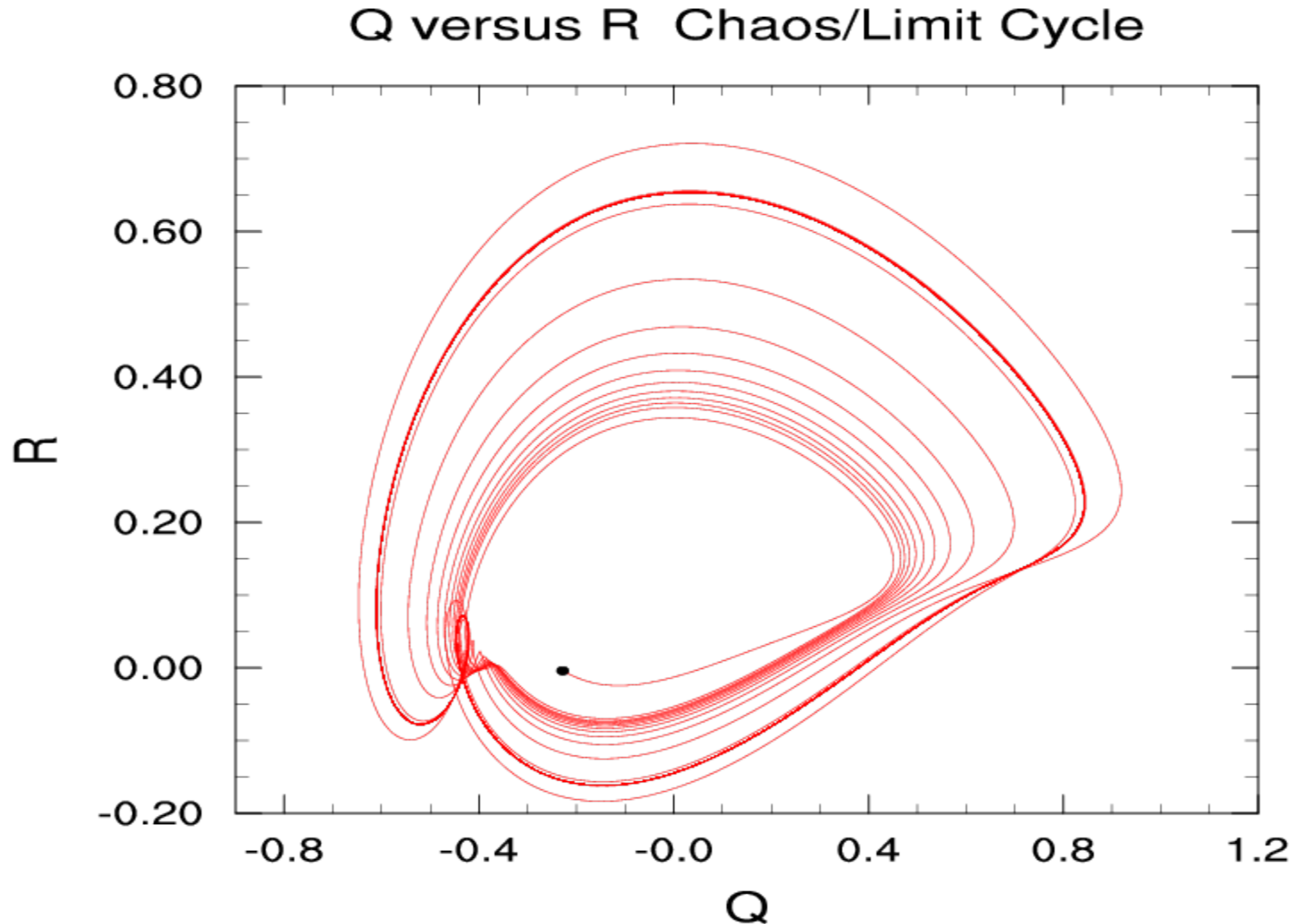


Figure 12. X(1) vs R for run (300,-34, 50, 50) Iterations only out to 16,000

**R2** passes the critical value of **0.88** at its 1<sup>st</sup> max. It increases in magnitude for 10 more cycles to **1.21**. As expected in chaos, X(1) grows with each cycle. At the 11<sup>th</sup> **R2** max it makes a large jump (**R2 = 1.43**) producing the **maximum loop of X(1)** shown in Figure above. **R** makes an extremely stable loop in response – along with **Q** (shown in the next slide)



**Figure 13. Q versus R Chaos/Limit Cycle run (300, -34, 50, 50)**  
Within the loop, there is a secondary **minimum of Q** and a secondary **maximum of R** creating a local minimum of the **[  $Q^3 - R^2$  ]** value

## Q versus R Chaos

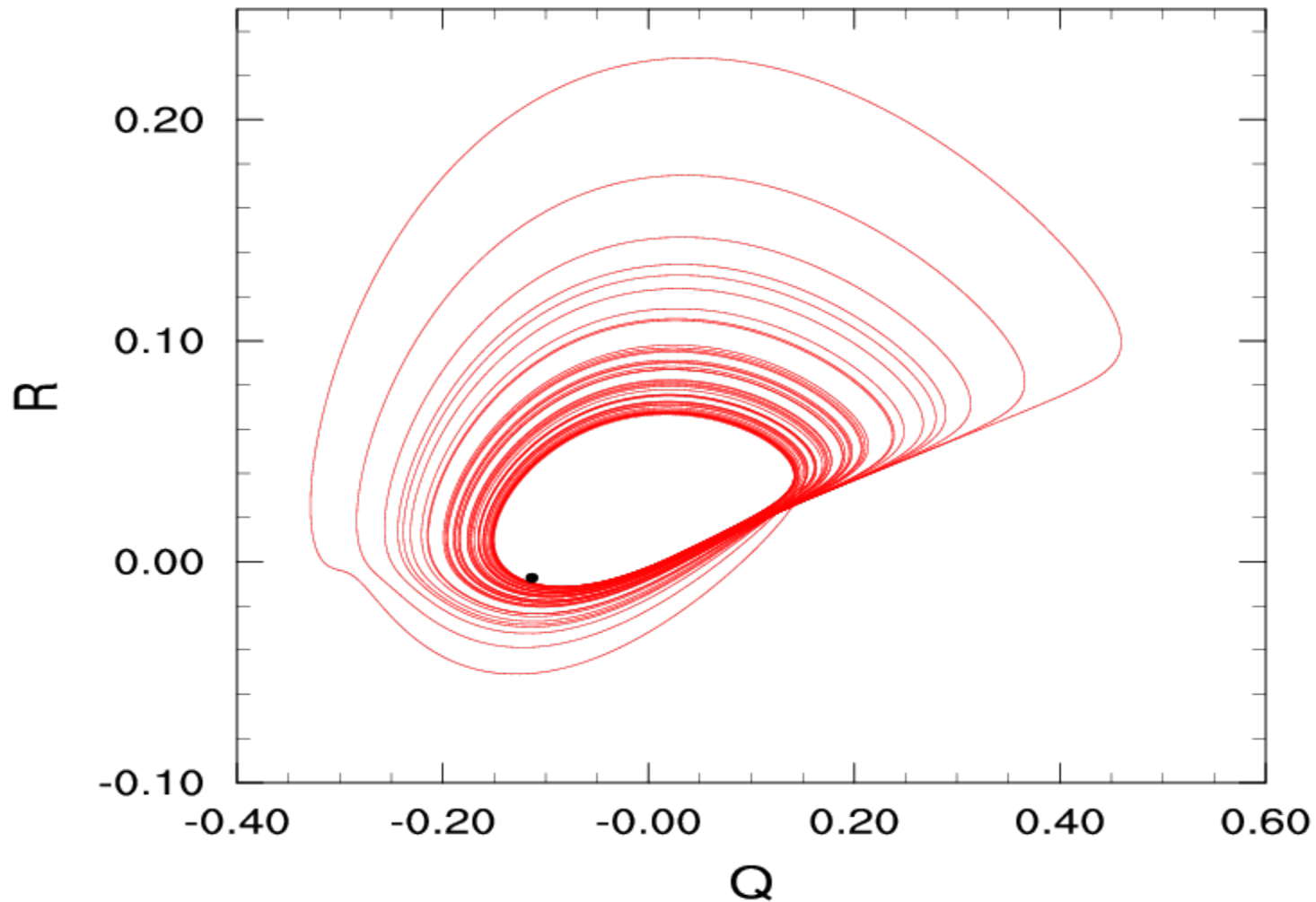


**Figure 5. Q versus R Chaos run (100, 0, 50, 50) Iterations = 100,000**  
**There is much wider range of Q compared to R**

## Sequence of events for the bifurcation from chaos to lock-in limit cycles

The extreme  $R_2$  maximum value, at its 11<sup>th</sup> cycle, kicks off the event by creating the extra large  $X(1)$  cycle

$X(1)$  becomes relatively large negative. Recall that  $X(1) = - [ R^2 + D^2 ]^{1/2}$  was an unstable and unphysical attractor – leading to negative kinetic energy

$X(1)$  &  $X(3)$  obtain values that cause  $Q$  &  $R$  to avoid this unphysical case

A secondary local minimum of  $Q$  and a local maximum of  $R$  (both extremely stable moves) put a loop in the  $Q$  versus  $R$  plane

This creates a local minimum in the  $[ Q^3 - R^2 ]$  value – delaying the subsequent breakout of the three root solution later in the baroclinic cycle

When the three root breakout does occur,  $R_2$  has a lower value than its previous breakout value

$R_2 = 1.34$  at its 12<sup>th</sup> maximum -- considerably lower than its 11<sup>th</sup> maximum of  $R_2 = 1.43$ . After two more cycles,  $R_2$  settles into its locked-in value of  $R_2 = 1.357$

### X3 vs R Chaos/Limit Cycle

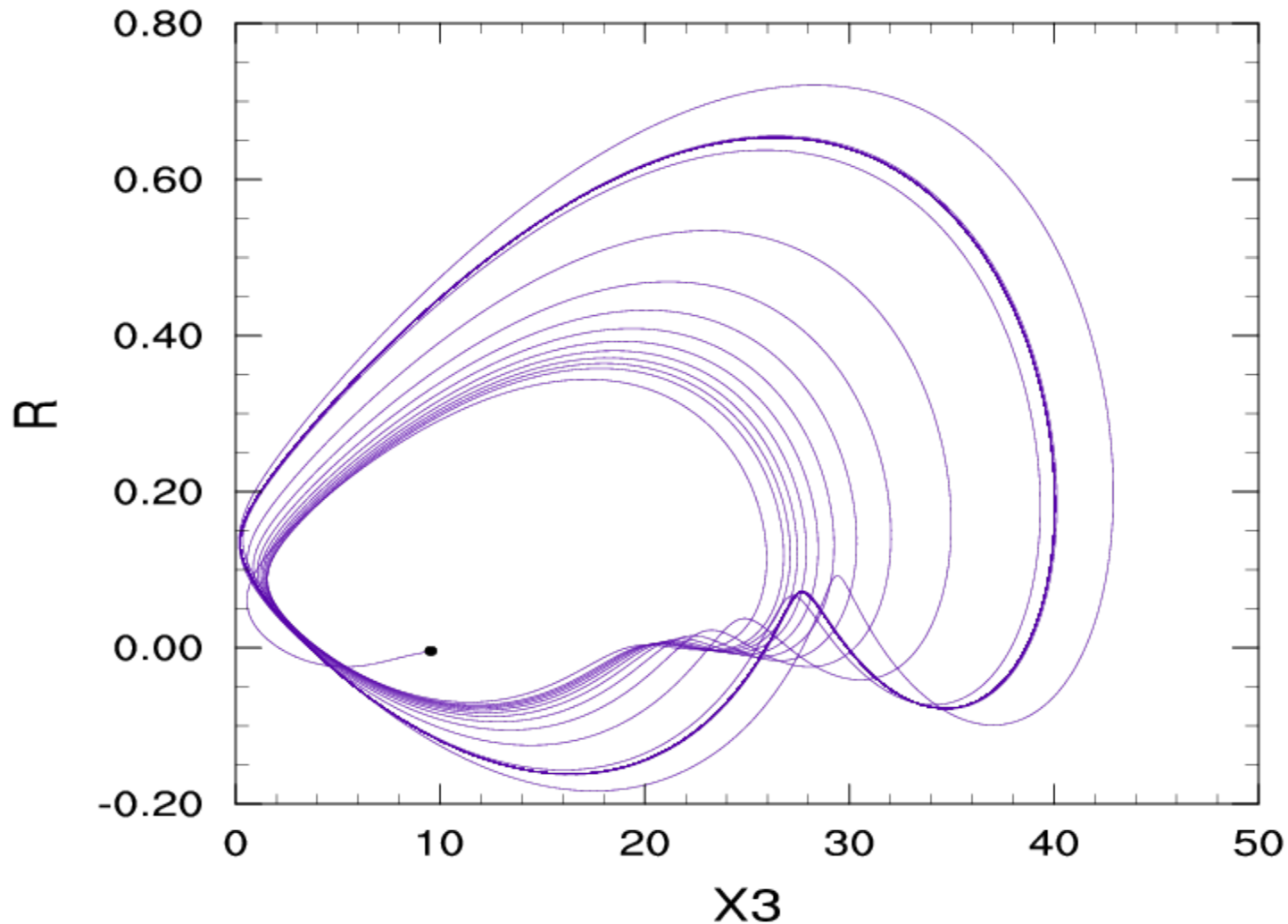


Figure 14. X3 versus **R** Chaos/Limit Cycle run (300, -34, 50, 50)  
X3 always positive and helps create **secondary R maximum**

**Had one progressed from a very high differential heating to today's differential heating rate one has a classic example of a route to chaos!**

**There are only **vacillation solutions** for  $IH \geq 356$**

**As  $IH$  comes down from 355 to 250 there is **single lock-in limit cycle****

**As  $IH$  proceeds from 250 to 200 there is a progression of bifurcations which lead to **two limit cycles** that have frequencies of **+ /- (0 to 294.5) iterations** from the bifurcation frequency – the longer period cycle has the greater change in the amplitude of the various variables**

**As  $IH$  continues lower below 200, the system is more unstable and **chaos occurs more frequently over a greater range of initial conditions****

**A precise value of the root R2 determines whether chaos occurs for each value of  $IH$  as it progresses lower.**

**The implication is that if  $IH$  were to continue to values lower than the current differential heating there would be more instances of chaos. We found this to be true; and even progressed to low heating and friction rates like Pedlosky (1987) studied and found similar results, but that is perhaps a subject for another talk**

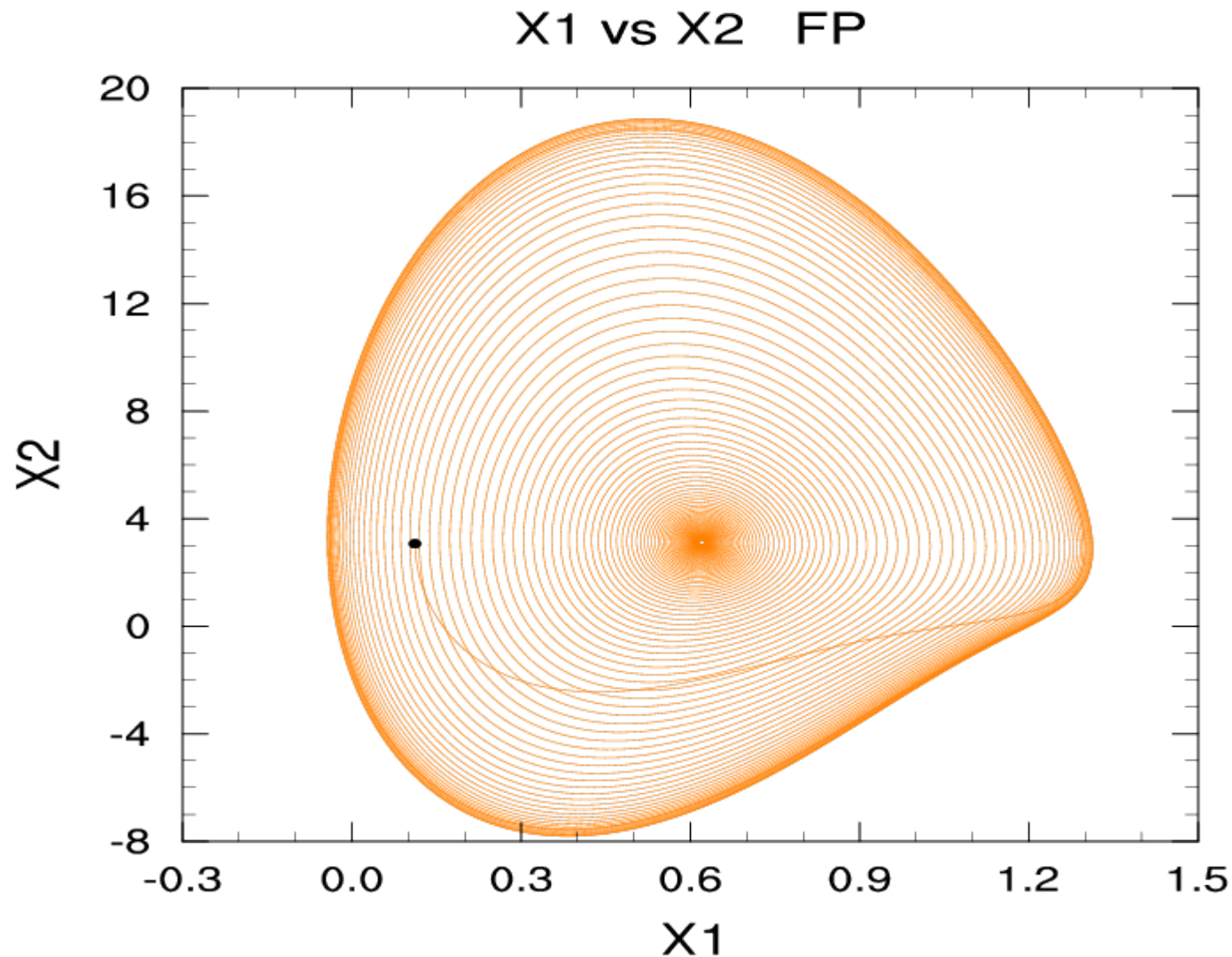


**Figure 15. X1 vs X2 vacillation / FP run (300, -32, 50, 50) Iterations = 100,000**  
**This demonstrates the magnitude of the vacillation cycle at very large IH values**  
**(compare  $X2 = \sim 4$  for  $IH = 100$  in Figure 1)**

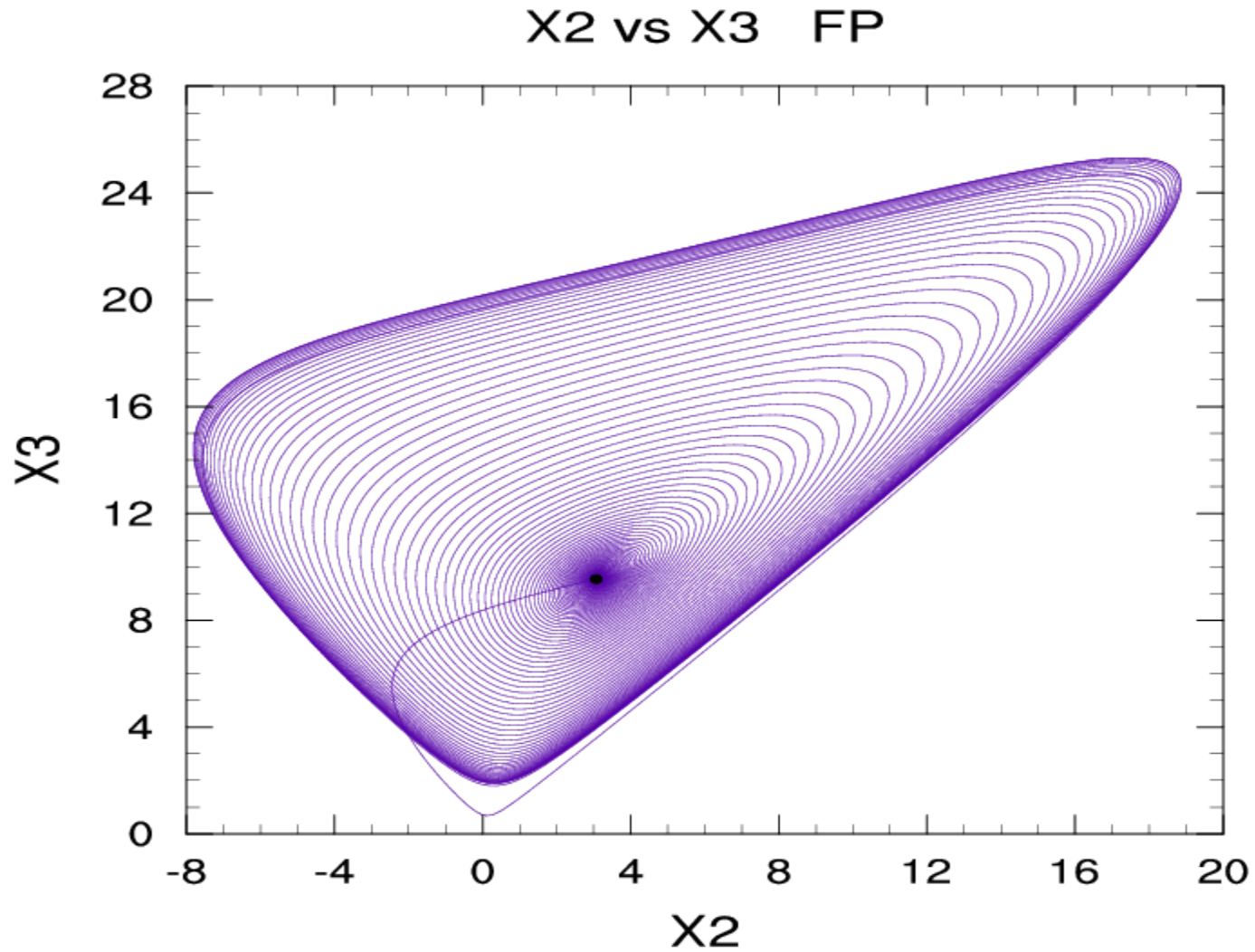
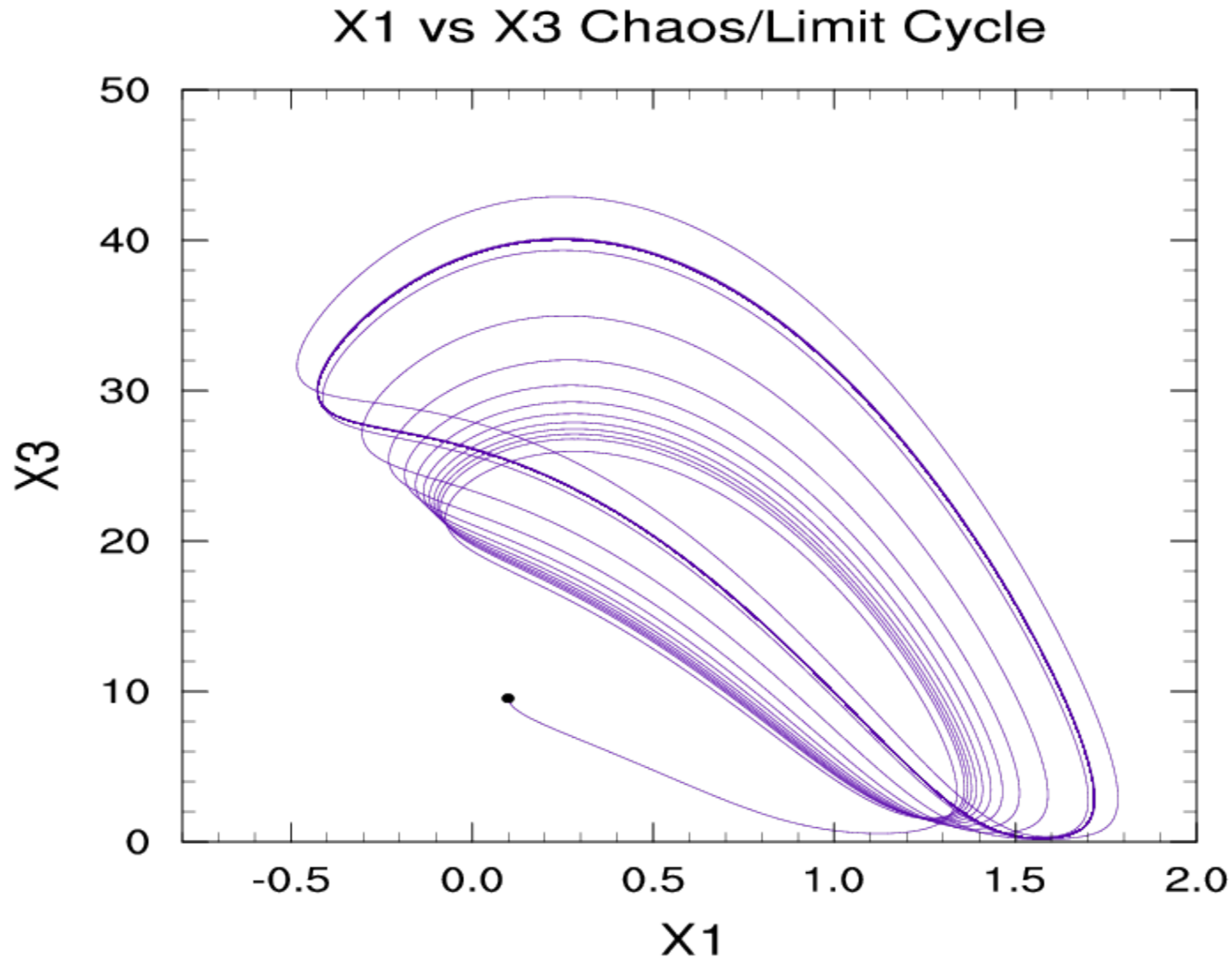


Figure 16. X2 vs X3 FP run (300, -32, 50, 50) Iterations = 100,000

**X(2) & X(3) start at FP values and return there – much action in between**



**Figure 17. X1 versus X3 Chaos/Limit Cycle run (300, -34, 50, 50)**

**The max meridional velocity here is 42.9 m/s – compare with 32.6 m/s for FP**

The maximum northward component of velocity (a proxy for relative storm intensity) shown in blue for FP and orange for chaos

T87 found the FP value of 11 m/s [ the same value of 11 m/s was found for the rms value at 500mb in the Southern Hemisphere summer by Oort (1983) ]

We have used the maximum value found in a solution to compare impact

IH	First FP/Chaos Boundary		Second FP/Chaos Boundary		Third FP/Chaos Boundary	
	(ISET)	Type	(ISET)	Type	(ISET)	Type
<b>100</b>	(-1) FP	(0) Chaos	(17) FP	(16) Chaos	(96) FP	(97) Chaos
V m/s	17.60	25.67	17.72	24.09	18.99	27.23
<b>120</b>	(-7) FP	(-6) Chaos	(12) FP	(11) Chaos	(104) FP	(105) Chaos
V m/s	19.78	26.57	19.58	27.73	21.19	28.85
<b>160</b>	(-19) FP	(-18) Chaos	(2) FP	(1) Chaos	(121) FP	(122) Chaos
V m/s	23.34	33.20	23.00	39.56	25.32	31.88
<b>180</b>	(-25) FP	(-24) Chaos	(-3) FP	(-4) Chaos	(129) FP	(130) Chaos
V m/s	24.81	36.96	24.62	40.93	24.96	37.93

For IH = 100, the range of increase of chaos over FP is 36% to 46% for these boundary cases. Randomly chosen cases not on the boundary show increases as high as 75%

FP solutions have much higher vacillation amplitude for increased differential heating

From the previous Table the middle column shows increase of heating  
From  $IH = 100$  to  $180$  causes a 39% increase in  $V$  ( $17.72$  vs  $24.62$ ) due to **vacillation amplitude increase**; a 70% increase in  $V$  ( $40.93$  vs  $24.09$ ) due to the **chaos**; comparing **chaos at  $IH = 180$**  with **vacillation at  $IH = 100$** , the increase in  $V$  is 131%.

**Such explosive baroclinic instability (EBI) is occasionally seen in today's times (not necessarily every year, nor with the same intensity within a year), when Arctic air is driven southward deep into Mexico**

**EBI may be one of the factors that influence the occurrence of some of the extreme weather events seen in modern times and in the recent past**

Several cold periods in the past (identified by Plimer, 2009): Bronze Age Cooling (3,200 - 2,500bp), the Dark Ages (535AD – 900AD), and the Little Ice Age (1300AD -- 1850AD) had stormier and windier conditions – **such were well documented in the Little Ice Age. Increased differential heating with chaotic periods would make these conditions far worse than today.**

At the beginning of **glacial conditions**, such extended cycles of storm intensity, **occurring at strategic periods of the seasonal cycle could be capable of building up enormous quantities of ground ice mass in the higher latitudes**